Original Article

Gene expression profiles for apoptotic and necrotic pathways during *Amanita phalloides* intoxication in mice

Selim Karahan[1,2] ⓘ, Zehra Atli[3] ⓘ, Ertugrul Kaya[4] ⓘ, Feride Ozdemir[5] ⓘ, Mehmet Boga[1,6] ⓘ, Sevcan Izgi[7] ⓘ

[1]Dicle University, Health Sciences Application and Research Center (DUSAM), Diyarbakir, Turkiye
[2]Dicle University, Faculty of Veterinary, Department of Laboratory Animals, Diyarbakir, Turkiye
[3]Dicle University, Faculty of Medicine, Department of Pharmacology, Diyarbakir, Turkiye
[4]Düzce University, Faculty of Medicine, Department of Pharmacology, Duzce, Turkiye
[5]Istanbul University, Faculty of Medicine, Department of Histology and Embryology, Istanbul, Turkiye
[6]Dicle University, Faculty of Pharmacy, Department of Analytical Chemistry, Diyarbakır, Turkiye
[7]Gaziantep University, Faculty of Medicine, Department of Medical Biology, Gaziantep, Turkiye

ORCID IDs of the authors: S.K. 0000-0001-5784-7091; Z.A. 0000-0001-8428-6779; E.K. 0000-0003-0081-682X; F.Ö. 0000-0003-1327-9146; M.B. 0000-0003-4163-9962; S.İ. 0000-0002-8799-2043

ABSTRACT

Background and Aims: *Amanita phalloides* is the deadliest toxic mushroom in the world and causes death from acute liver failure. α-amanitin (α-AMA), the most potent toxin, inhibits RNA polymerase II in hepatocytes, stops protein synthesis, and causes hepatotoxicity. However, the information about the mechanisms underlying hepatotoxicity caused by α-AMA is quite inadequate. This study aims to reveal the complex necrotic and apoptotic mechanisms occurring in mouse hepatocytes depending on *A. phalloides* exposure time *in vivo*.

Methods: BALB-c male mice were divided into 5 groups (n=7): control, α-AMA-2, α-AMA-12, α-AMA-72, and α-AMA-96 groups. A poisoning model was created by oral administration of *A. phalloides* mushroom extract containing 10 mg/kg of α-AMA to mice and they were sacrificed after 2, 12, 72, and 96 h. Then, *TNF-α, Bax, caspase-3*, and *Bcl-2* gene expression levels in liver tissues were examined by the RT-qPCR method. Time-dependent damage to liver tissues was also evaluated histopathologically.

Results: RT-qPCR results showed that proinflammatory cytokine TNF-α mRNA expression levels increased in mouse liver tissues at 2 and 12 h after *A. phalloides* administration compared among the groups. *Bax* mRNA expression levels increased in the 12 and 72 h after *A. phalloides* ingestion. It was observed that *caspase*-3 mRNA expression levels increased in the 72 and 96 h groups compared among the groups, while *Bcl*-2 mRNA expression levels decreased in the 72 and 96 h groups.

Conclusion: Our findings showed that necrotic mechanisms develop in the early period after *A. phalloides* mushroom poisoning, and then apoptotic mechanisms are effective. In conclusion, understanding the mechanisms of *A. phalloides*-induced hepatotoxicity will provide important information for new treatment strategies to be developed.

Keywords: α-amanitin, *TNF-α, Bax, caspase-3, Bcl-2*, RT-qPCR

Address for Correspondence:
Selim KARAHAN, e-mail: slmkarahan@gmail.com

INTRODUCTION

Amanita phalloides (Vaill.) Link species is the deadliest toxic mushroom in the world, resulting in acute liver failure, and is responsible for more than 90% of deaths from mushroom poisoning worldwide (Vetter, 1998). The clinical properties of *A. phalloides* poisoning are the development of liver necrosis, which leads to the development of the hepatorenal phase. Patients gradually lose their liver and kidney functions, and hypoglycemia, delirium, and confusion may develop (Becker et al., 1976). Approximately 20-79% of poisoned patients develop chronic liver disease, but it is unknown how many *A. phalloides* consumed are lethal to humans (Serné et al., 1996; Yilmaz, Ermis, Akata, & Kaya, 2015).

There is typically a 6-24 h delay between ingestion of the mushrooms and the onset of gastrointestinal symptoms (GIS) (latency phase). The first symptoms are GIS complaints and the symptoms may persist for several days. During the next 24-36 h, acute hepatic failure and subsequent multi-organ injury are revealed by both clinical and laboratory measurements (hepato-renal phase) (Escudié et al., 2007; Karlson-Stiber & Persson, 2003). In fatal poisonings, death usually occurs after 5 or 6 days (median time is 6.1 days) (Ganzert, Felgenhauer, & Zilker, 2005). The severity of poisoning seems to be related to the amount of toxin taken in proportion to body weight (Enjalbert et al., 2002; Jan, Siddiqui, Ahmed, Ul Haq, & Khan, 2008). The severity of liver damage, the rate of hepatic regeneration, and an effective treatment of poisoning increase the survival rate of patients (Alldredge B, 2012). Currently, no radical treatment has been found for *A. phalloides* mushroom poisoning (Garcia et al., 2015).

Amatoxins are known as the toxins responsible for fatal mushroom poisoning and are mainly responsible for the severe liver damage observed after *A. phalloides* poisoning (Yilmaz et al., 2015). α-amanitin (α-AMA) is the most toxic substance among amatoxins and it is a bicyclic octapeptide compound with high molecular weight, heat stability, and water solubility (Kaya E, 2012; Wieland & Faulstich, 1978). α-AMA has been the most known and causes hepatocellular failure due to hepatotoxicity. The main toxic mechanism of α-AMA is non-competitive nuclear inhibition of RNA polymerase II in eukaryotic cells, thereby inhibiting protein synthesis. As a transcription inhibitor, α-AMA disrupts/stops many mechanisms in cells. Decreased mRNA levels lead to decreased protein synthesis, the development of necrotic mechanisms, and ultimately cell death (Lindell, Weinberg, Morris, Roeder, & Rutter, 1970; Wieland, 1983).

Apoptosis is the orderly programming of cell death during normal development and is controlled by different intrinsic regulatory pathways. Mechanisms that inhibit DNA transcription, such as α-AMA, induce cell cycle arrest or apoptosis in response to certain cellular stresses. α-AMA is a potent inducer of apoptosis, and apoptotic mechanisms are thought to play an important role in the pathogenesis of hepatic injury during *A. phalloides* poisoning (Y. Arima et al., 2005). *In vitro* studies have shown that apoptosis may play an important role in severe α-AMA-induced liver injury, as observed in canine primary hepatocytes (Magdalan, Ostrowska, Piotrowska, Izykowska, et al., 2010) and human hepatocyte cultures

(Magdalan, Ostrowska, Piotrowska, Gomułkiewicz, et al., 2010; Magdalan et al., 2011). It has been reported that α-AMA induces apoptosis by acting synergistically with tumor necrosis factor-α (*TNF-α*), but the underlying mechanisms are not yet known. Also, α-AMA initiates apoptotic mechanisms by inducing p53 protein, which triggers apoptosis (Y. Arima et al., 2005). It has also been suggested that destroying the mitochondrial membrane potential is important in the development of severe hepatotoxicity by α-AMA (Wang et al., 2018). It has been reported that after high-dose α-AMA *in vivo* administration, it increases hepatic pro-inflammatory *TNF-α* mRNA levels, apoptosis develops in hepatocytes, and liver damage is prevented in mice treated with anti-TNF-α antibodies (Leist et al., 1997). However, the dependence of α-AMA toxicity on the presence of *TNF-α* has not been confirmed in another study using hepatocyte cultures (Magdalan, Ostrowska, Piotrowska, Izykowska, et al., 2010). *TNF-α* induces hepatocellular apoptosis but it has also been reported to induce necrosis in *in vivo* models of inflammatory liver injury (Tiegs & Horst, 2022). Induction of necrosis and apoptosis by α-AMA is a complex process and understanding the cellular processes that cause liver injury is clinically crucial.

Today, there is still an increase in cases of poisoning caused by deadly mushrooms and, a radical treatment has not yet been found for *A. phalloides* intoxication (Ertugrul Kaya et al., 2016). Commonly used treatments are carried out only with palliative treatment. The development of effective new therapeutic alternatives is extremely important to improve the survival of patients poisoned with *A. phalloides*. Thus, this study aimed to investigate the complex apoptotic [*Bax* (Bcl-2-associated X protein), *caspase-3* (cysteine-aspartic acid protease-3) and *Bcl-2* (B-cell lymphoma-2)] and necrotic [*TNF-α* (tumor necrosis factor-α)] mechanisms at the gene expression levels that occur in mouse hepatocyte cells based on exposure time to α-AMA cytotoxicity. In this way, the molecular mechanisms underlying hepatic damage caused by α-AMA have been attempted to be clarified. Thus, our findings may contribute to developing new treatment strategies for patients poisoned by *A. phalloides*.

MATERIAL AND METHODS

A. phalloides mushroom collection
A. phalloides mushrooms were collected from the forest areas of Gümüşova (Düzce, Türkiye). The collected mushrooms were systematically identified by examining their macroscopic properties (Figure 1).

A. phalloides mushroom extraction
Mushrooms were dried under 50-60°C airflow for 24 h and ground into powder. Ten grams of *A. phalloides* was placed in 150 mL solvent (methanol, water, 0.01 M HCl (5:4:1, v/v/v), homogenized with a sonicator, and incubated for 24 h. Then, the solution was centrifuged for 5 min at 5000 rpm and the supernatant was filtered by syringe filters (0.22 μL) and extracted in 150 mL of 50% methanol for 4 h in a Soxhlet apparatus. The obtained extracts were evaporated in a vacuum evaporator at 50°C until completely dry (E. Kaya et al., 2015).

Determination of quantity of α-AMA

In the analytical HPLC system, an α-AMA standard (1 mg/mL, Sigma Aldrich, St. Louis, MO, USA) was diluted in dH_2O at 10, 20, 100, 200, 1000, and 2000 ng/mL concentrations, and a 6-point calibration curve (repeated 3 times) was created. The calibration curve was linear over the desired concentrations ($R^2 > 0.99$). The chromatographic method was performed as reported by Kaya et al (E. Kaya et al., 2015; E. Kaya et al., 2013). Analysis of the mushroom extract was performed on a Reversed-Phase High-Performance Liquid Chromatography system (RP-HPLC, Shimadzu, Japan) and RP-HPLC conditions were as follows: 150 x 4.6 mm, 5 µm particles, C18 column (Agilent Technologies, Palo Alto, CA) with 302 nm at the DAD detector. The mobile phase [0.05 M ammonium acetate (pH 5.5)/acetonitrile (90:10 v/v)] was used with 1 mL/min flow rate. The detection limit was determined as 2 ng/g and the amount of α-AMA was calculated as the mean ± SEM in 1 g of dry mushroom.

Briefly, 1 mL of the *A. phalloides* water extract was applied to the semi-preparative RP-HPLC. From the beginning to the end of the peak at the same retention time as the α-AMA standard, the fraction was collected by the collector (4.6 x 250 mm C18 ODS column with 5 µm particles was used). The obtained fraction was dried in a vacuum evaporator at 50°C, dissolved in 1 mL of 40% methanol, and reapplied to the preparative HPLC system for the second purification. Then, 20 µL of α-AMA was applied to the analytical HPLC system to measure the purity and amount of toxin in that fraction.

The amount of substance was measured by applying the peak areas obtained in the analysis to the equation of the calibration curve. The obtained pure α-AMA was dissolved in 1 mL distilled water after the solvent was evaporated, and quantitative analysis was performed. Based on analysis of the results obtained, *A. phalloides* extracts dissolved in distilled water containing 20 mg of α-AMA were prepared.

Animals and treatments

Male BALB-c mice (weighing 20-30 g) were obtained from Dicle University Health Sciences Application and Research Center (DÜSAM). The permission of Dicle University Experimental Animals Local Ethics Committee (DUHADEK-2021/45) was obtained and all animal experiments were performed according to the instructions of the Local Ethics Committee. The animals were housed under conditions of constant temperature (22±3°C) and humidity (50-55%), a 12 h light/dark cycle, and free access to food and water. After a 1-week adaptation period, the animals were randomly divided into five groups (n = 7).

The animal model of intoxication has been used as a reliable model for α-AMA poisoning, since it shows similar hepatotoxic effects after amatoxin administration in humans (Tong et al., 2007; Zhao et al., 2006). In addition, toxin concentrations and experimental design in the *in vivo* study were designed from a clinical perspective, based on available information on clinical toxicity practices and α-AMA pharmacokinetics. The experimental design is shown in Figure 2. *A. phalloides* mushroom water extract was given orally through stomach gavage at a concentration of 10 mg/kg α-AMA (Garcia et al., 2015; Park et al., 2021; Wieland & Faulstich, 1978). Mice were starved for 24 h before the start of the experiments. In the control group, a single dose of 1 mL of 0.9% physiological saline was administered to the mice via orogastric gavage at 0 min. In the α-AMA-2, α-AMA-12, α-AMA-72, α-AMA-96 groups, *A. phalloides* mushroom water extract, which included 10 mg/kg α-AMA, was
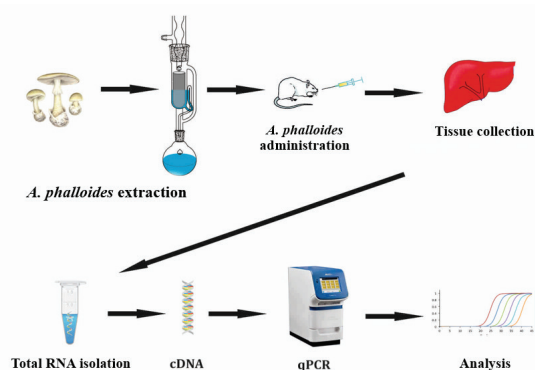

Figure 1. *Amanita phalloides.*

Figure 2. Experimental Design.

Table 1. Primer sequences		
Gene	**Forward primer (5′–3′)**	**Reverse primer (5′–3′)**
Bax	GGATGCGTCCACCAAGAAG	GGAGGAAGTCCAGTGTCCAGCC
Bcl-2	TGAGTACCTGAACCGGCATCT	GCATCCCAGCCTCCGTTAT
caspase-3	TGCAGAACAAAACCTCAGT	TGTCTCTCTGAGGTTGGCTG
TNF-α	AAATGGGCTCCCTCTCATCAGTTC	TCTGCTTGGTGGTTTGCTACGAC
GAPDH	ACTCCACTCACGGCAAATTC	TCTCCATGGTGGTGAAGACA

administered to the mice via orogastric gavage at 0 min. The animals were sacrificed and their livers were taken at 2, 12, 72, and 96 h, respectively. At the end of the experiments, the mice were sacrificed under anesthesia [Ketamine (90mg/kg) + Xylazine (10mg/kg)]. The liver tissues were stored at -80°C for RT-qPCR analysis. A part of the liver was also fixed in 10% zinc-formalin solution for 24 h and then embedded in paraffin for routine histopathologic analysis.

Quantitative real-time polymerase chain reaction (RT-qPCR) assay

To investigate the molecular mechanisms of apoptotic and necrotic pathways caused by *A. phalloides*, *TNF-α*, *Bax*, *caspase-3* and *Bcl-2* gene expression levels were measured by Real Time-Polymerase Chain Reaction (RT-qPCR, Applied Bioscience StepOnePlus™, Foster City, CA). RNA purification was performed from liver tissues stored at -80°C. Total RNA was isolated from tissues using RiboZol™ (VWR-Amresco, USA) according to the manufacturer's instructions. The quantity and quality of RNA samples were measured using a microvolume spectrophotometer (Nano-Drop 2000C, Thermo Scientific, USA). Genomic DNA contamination was removed with the DNAse-I digestion enzyme (Thermo Fisher, USA). cDNA synthesis was performed using the cDNA Synthesis Kit (Thermo Fisher, USA) according to the manufacturer's instructions. The sequences of primer pairs used for qPCR analysis were designed using Primer3 software and based on the sequences in the NCBI database (Table 1). For RT-qPCR amplification, a 20 μL volume of reaction mix was prepared with 10 μL of 2X SYBR Green Master Mix, 0.2 μm primer, and 1 μL of cDNA. Real-time PCR thermal cycling conditions were performed by initial denaturation at 95°C for 10 min, followed by 40 cycles of denaturation at 95°C for 30 sec, 1 min reassembly at 60°C, and an extension period for 30 sec at 72°C. Melting curve analysis was performed by increasing the temperature by 1°C at each step from 55°C to 95°C. Samples without cDNA were used as a negative control. The housekeeping gene (GAPDH) expression was used as an internal control for normalization. For each cDNA sample, PCR amplifications were performed in triplicate and relative mRNA expressions were evaluated by the comparative Ct method ($2^{-\Delta\Delta CT}$) described by Schmittgen & Livak (Schmittgen & Livak, 2008).

Histopathological assessment

For light microscopic evaluation, liver tissue samples were fixed in 10% formaldehyde and embedded in paraffin. Then, 5-μm-thick sections were cut from the paraffin-embedded samples, mounted on slides, and stained with hematoxylin and eosin (H-E). The tissue samples were examined using a light microscope. The sections were evaluated for liver damage such as inflammation, sinusoidal dilatation, necrosis, congestion, and pyknotic nucleus.

Statistical analysis

The One-way ANOVA was performed with the IBM SPSS Statistics 24.0 (IBM Inc, Chicago, IL, USA) statistical software. Post hoc Tukey test was used for between-group comparison of *Bax*, *Bcl-2*, *caspase-3*, and *TNF-α* gene expressions. The data of this study are given as the mean ± SEM. A value of $p<0.05$ was accepted as statistically significant among groups.

RESULTS

The retention times for β-AMA, α-AMA, and γ-AMA in the RP-HPLC chromatogram were 4.818, 6.219 and 12.577 min respectively. The RP-HPLC chromatogram of α-AMA analysis is given in Figure 3.

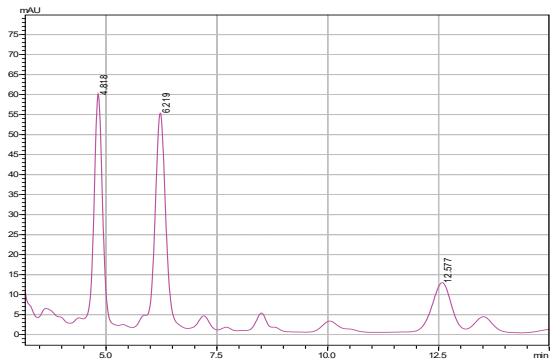## Time-dependent expression of *TNF-α*, *Bax*, *caspase-3*, and *Bcl-2* genes after *A. phalloides* administration

Figure 3. Analytical HPLC chromatograms of α-AMA.

The results of RT-qPCR clearly showed that pro-inflammatory cytokine *TNF-α* mRNA expression was increased in α-AMA-2 ($p < 0.01$) and α-AMA-12 ($p < 0.05$) groups after *A. phalloides* administration (Figure 4), suggesting that exposure to *A. phalloides* induces inflammation in hepatocytes. *TNF-α* expression at the mRNA levels decreased gradually at α-AMA-72 and α-AMA-96 groups after *A. phalloides* administration compared to the α-AMA-2 group.

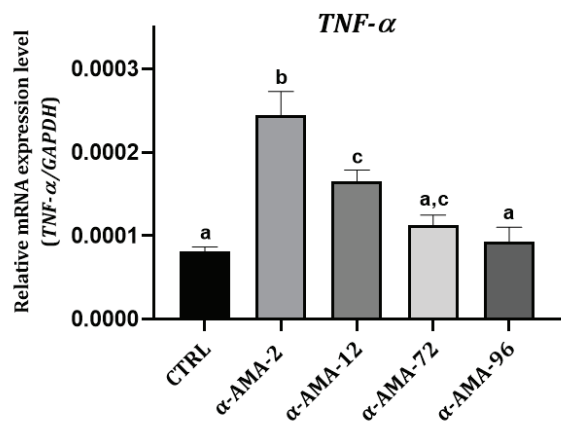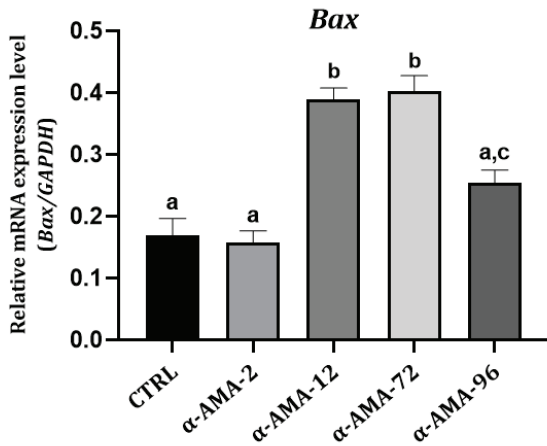While *Bax* mRNA expression level was upregulated in the α-AMA-12 and α-AMA-72 groups compared to the control

Figure 4. Time-dependent expression of *TNF-α* gene after *A. phalloides* administration. Mice were treated with *A. phalloides* extract including 10 mg/kg α-AMA. *TNF-α* gene expression was analyzed by RT-qPCR. Different letters mean significant differences between groups. [b]$p < 0.01$ compared to control, α-AMA-72 and α-AMA-96 groups; [c]$p < 0.05$ compared to control, α-AMA-2 and α-AMA-96 groups.

group and α-AMA-2 ($p < 0.01$), expression of the *Bax* gene was downregulated in the α-AMA-96 group compared to the α-AMA-12 and α-AMA-72 groups ($p < 0.01$) (Figure 5). These results indicate that apoptosis is induced 12 h after *A. phalloides* administration compared to that in healthy untreated mice. However, *Bax* mRNA expression level decreased at 96 h after *A. phalloides* administration.

Additionally, it was observed that the pro-apoptotic marker *cas-*

Figure 5. Time-dependent expression of *Bax* gene after *A. phalloides* administration. Mice were treated with *A. phalloides* extract including 10 mg/kg α-AMA. *Bax* gene expression was analyzed by RT-qPCR. Different letters mean significant differences between groups. [b]$p < 0.01$ compared to control, α-AMA-2 and α-AMA-96 groups; [c]$p < 0.05$ compared to α-AMA-2 groups.
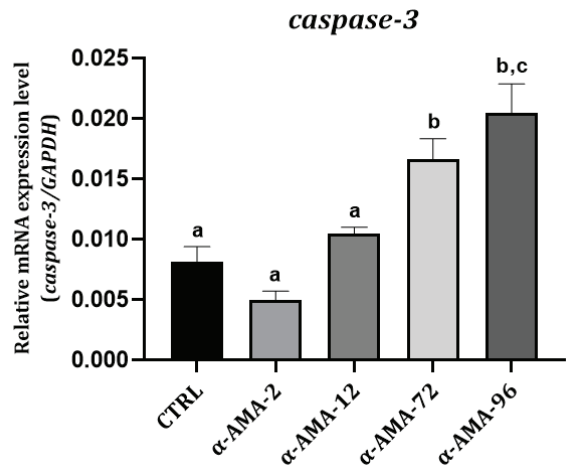
pase-3 mRNA expression level decreased in the α-AMA-2 group compared to the control group, but it was not statistically significant. Administration of *A. phalloides* significantly enhanced the mRNA expression of the *caspase-3* in the α-AMA-72 ($p < 0.05$) and α-AMA-96 groups ($p < 0.01$) (Figure 6).

There were only decreased expression profiles for the anti-apoptotic marker *Bcl-2* in the α-AMA-72 and α-AMA-96 groups, compared among the groups ($p < 0.05$ and $p < 0.01$) (Figure 7).
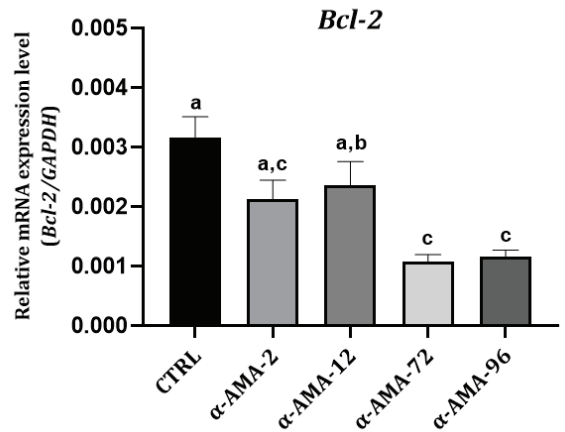
Time-dependent histopathological examinations after *A. phalloides* administration

No pathological observations were seen for liver tissue in the control group. Hepatic cells and the central vein exhibited normal histological appearances as shown in Figure 8-a. In the α-AMA-2 group, sinusoidal dilatation and hepatocytes with the pyknotic nucleus were observed (Figure 8-b). The liver tissues of the α-AMA-96 group showed prominent portal and lobular changes including vascular congestion, inflammation, necrosis, sinusoidal dilatation, and hepatocytes with pyknotic nucleus (Figure 8-c). Histopathological changes observed in the α-AMA-2 group were milder than in the α-AMA-96 group (Figure 8: a, b, c: H&E staining; x20 magnification).

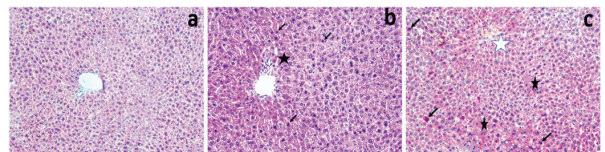### DISCUSSION

Figure 6. Time-dependent expression of *caspase*-3 gene after *A. phalloides* administration. Mice were treated with *A. phalloides* extract including 10 mg/kg α-AMA. *caspase-3* gene expression was analyzed by RT-qPCR. Different letters mean significant differences between groups. [b]$p < 0.05$ compared to control, α-AMA-2 and α-AMA-12 groups; [c]$p < 0.01$ compared to control, α-AMA-2 and α-AMA-12 groups.

Figure 7. Time-dependent expression of *Bcl-2* gene after *A. phalloides* administration. Mice were treated with *A. phalloides* extract including 10 mg/kg α-AMA. *Bcl-2* gene expression was analyzed by RT-qPCR. Different letters mean significant differences between groups. [a]$p < 0.01$ compared to α-AMA-72 and α-AMA-96 groups; [b]$p < 0.05$ compared to α-AMA-72 and α-AMA-96 groups.

Figure 8. Histopathologic assessments. Mice were treated with *A. phalloides* extract including 10 mg/kg α-AMA. **a)** Liver tissue showed normal histological appearance with hepatic cells and central vein in the control group. **b)** Sinusoidal dilatation (black asterisks) and hepatocytes with pyknotic nucleus (black arrows) were observed in the α-AMA-2 group. **c)** In the α-AMA-96 group severe necrosis with the disappearance of nuclei (black asterisks), sinusoidal dilatation (white asterisks), and hepatocytes with pyknotic nucleus (black arrows) were observed. a, b, c: H&E; x20.

There is no clinical antidote for *A. phalloides* poisoning and symptomatic treatment is the only option (Garcia et al., 2015). α-AMA, the most potent toxin in *A. phalloides,* irreversibly inhibits RNA polymerase II in hepatocytes and inhibits protein synthesis. The liver is the most affected by α-AMA because of the high protein synthesis and regeneration. Hepatic damage is exacerbated by the accumulation of α-AMA in liver tissues and undergoing enterohepatic circulation (Faulstich, Talas, & Wellhöner, 1985; Smith & Davis, 2016). In a study by Arima et al., it was shown that administration of α-AMA (2 μg/mL) for 24 h significantly induced p53 in fibroblast and HCT116 human colon carcinoma cells (Yoshimi Arima et al., 2004). In addition, it has been reported that α-AMA induces P53 protein to bind to anti-apoptotic Bcl-2 and Bcl-XL proteins independent of RNA polymerase inhibition and triggers apoptosis by causing cytochrome c to migrate from mitochondria to the cytosol (Y. Arima et al., 2005). Magdalan et al. reported that apoptosis induced by α-AMA in canine primary hepatocyte cells may contribute to the pathogenesis of severe liver damage, particularly in the early stages of poisoning (Magdalan, Ostrowska, Piotrowska, Izykowska, et al., 2010). Likewise, it has been reported that p53 and caspase-3-dependent apoptosis develops in hepatocyte cells exposed to α-AMA (2 μM) (Magdalan et al., 2011). On the other hand, in another *in vitro* study, L-amino-acid oxidase isolated from *A. phalloides* increased the Bax/Bcl-2 ratio by inducing caspase-dependent apoptosis in Jurkat cells, and then increased caspase-3 and caspase-9 protein expression (Pišlar, Sabotič, Šlenc, Brzin, & Kos, 2016). It has been revealed that the L-amino-acid oxidase enzyme also plays a role in the apoptotic mechanisms developing in *A. phalloides* poisoning.

Recent studies have shown that inflammatory cytokines such as TNF-α may induce local inflammatory mechanisms and ultimately lead to liver damage (Li et al., 2020). Fatal acute liver failure after *A. phalloides* ingestion can cause hepatocyte necrosis by inhibiting the synthesis of structural proteins (Angioi et al., 2021). Patient symptoms and clinical analyses show that acute tubular necrosis occurs with renal failure. In animals, 48 h after intravenous administration of α-AMA (0.327 mg/kg), tubular necrosis was observed in BALB/c mice (Zhao et al., 2006). Besides its role in inflammatory mechanisms, TNF-α has an important role in directly activating the extrinsic apoptotic pathway (Zhang et al., 2013). *TNF-α* mRNA levels were shown to increase concomitantly with hepatocyte apoptosis after administration of α-AMA (3 mg/kg i.p.) to mice (Leist et al., 1997). These studies show that *TNF-α* plays a role in both necrotic and apoptotic mechanisms after *A. phalloides* poisoning. The current study found that pro-inflammatory cytokine *TNF-α* mRNA levels increased in the early stage after *A. phalloides* administration (Figure 4), and increasing *TNF-α* mRNA levels tended to decrease at 72 and 96 h. These results indicate that caspase-independent necrotic mechanisms may play a role through the pro-inflammatory cytokine *TNF-α* in the early stages of poisoning. Activation of caspase-independent necrotic pathways may also trigger necroptotic mechanisms. Further studies on genes related to necroptosis will contribute to the emergence of necrotic mechanisms caused by α-AMA in liver tissues. Therefore, hepatic inflammation developing in the acute phase may be effective in the pathogenesis induced

by *A. phalloides*, but the effect of *TNF-α* on the apoptotic and necrotic mechanisms remain unclear. More studies are needed to define the crosstalk between inflammation, apoptosis and necrosis mechanisms in *A. phalloides* poisoning.

In the present study, pro-apoptotic *caspase-3* mRNA expression level was significantly increased at 72 and 96 h after *A. phalloides* administration, however, no significant change was observed in *caspase-3* mRNA levels after 2 and 12 h (Figure 6). Deregulation of caspases triggers cell death (McIlwain, Berger, & Mak, 2013). Increased *caspase-3* mRNA levels result in the rapid induction of apoptosis, and our results show that apoptosis is elevated 72 h after *A. phalloides* administration. These results may indicate the late onset of apoptosis (Zhou et al., 2017). Thereby, our findings suggest a critical role of *caspase-3* in *A. phalloides*-induced hepatotoxicity. In addition, it was observed that pro-apoptotic *Bax* mRNA levels increased 12 and 72 h after *A. phalloides* administration, while anti-apoptotic *Bcl-2* mRNA levels decreased after 12 and 72 h (Figure 5, Figure 7). As the *Bax/Bcl-2* ratio indicates the balance between the pro-and anti-apoptotic mRNA levels (Barbosa, Machado, Skildum, Scott, & Oliveira, 2012), our results suggest that apoptotic mechanisms play an effective role approximately 12 h after *A. phalloides* ingestion.

The severity of liver injury and the rate of hepatic regeneration are important factors that determine the survival of individuals. In the early study on hepatotoxicity in *A. phalloides* poisoning, massive hepatic central lobular cell necrosis was reported (Fineschi, Di Paolo, & Centini, 1996). Likewise, it was observed that mice poisoned with α-AMA (0.6 mg/kg i.p.) developed higher percentages of hepatonecrosis compared to the control group (Tong et al., 2007). In a study by Kaya et al., vacuolar degeneration was observed at 1 and 6 h in mouse liver tissues after α-AMA (1 mg/kg i.p.) administration, while Councilman-like structures and pycnotic cells were observed after 24 h (E. Kaya et al., 2014). Similarly, in a study by Garcia et al., it was reported that α-AMA (0.33 mg/kg i.p.) caused significant hepatic cellular edema, cytoplasmic vacuolization and interstitial inflammatory cell infiltration in mouse liver tissues 24 h after administration (Garcia et al., 2015). In our study, the results were similar to the literature. Sinusoidal dilatation and pyknotic nucleus were observed 2 h after *A. phalloides* ingestion (Figure 8-b). After 96 h, it showed prominent portal and lobular changes, including vascular occlusion, inflammation, necrosis, sinusoidal dilatation, and hepatocytes with pycnotic nuclei (Fig. 8-c).

CONCLUSION

In the current study, the mRNA expression of *Bax*, *caspase 3*, *Bcl-2*, and *TNF-α* were examined to investigate time-dependent apoptotic and necrotic mechanisms occurring in mouse liver tissues after *A. phalloides* administration. Pro-apoptotic, anti-apoptotic, and pro-inflammatory mRNA expression profiles evaluated by RT-qPCR show that *A. phalloides* induces necrotic mechanisms in the early phase of intoxication and then causes cell death through apoptotic mechanisms. Consequently, we have proven that apoptotic mechanisms play an essential role in the pathogenesis of *A. phalloides*-induced hepatotoxicity, and necrosis is also essential in the pathogenesis

of *A. phalloides*-induced hepatotoxicity during the early stage after ingestion. Our results have demonstrated for the first time that investigation of time-dependent apoptotic and necrotic mechanisms in mice will provide critical knowledge for further studies on the signaling pathways underlying hepatotoxicity from *A. phalloides*.

Peer-review: Externally peer-reviewed.

Informed Consent: Written consent was obtained from the participants.

Author Contributions: Conception/Design of Study- S.K., Z.A., E.K., F.Ö.; Data Acquisition- S.K., Z.A., E.K., F.Ö., S.İ.; Data Analysis/Interpretation- S.K., Z.A., E.K., M.B., F.Ö.; Drafting Manuscript- S.K., Z.A., F.Ö., S.İ.; Critical Revision of Manuscript- E.K., M.B.; Final Approval and Accountability- S.K., Z.A., E.K., F.Ö., M.B., S.İ.

Conflict of Interest: The authors have no conflict of interest to declare.

Ethics committee approval: Animal experimental procedures were conducted in accordance with animal study protocols approved by the Dicle University Animal Experiments Local Ethics Committee (DUHADEK-2021/45).

REFERENCES

- Alldredge B, C. R., Ernst M, Guglielmo B, Jacobson P, Kradjan, WA, & Williams, BR. (2012). *Koda-Kimble and Young's applied therapeutics: The clinical use of drugs* (K. W Ed. 10th edition ed.): Lippincott Williams & Wilkins.

- Angioi, A., Floris, M., Lepori, N., Bianco, P., Cabiddu, G., & Pani, A. (2021). Extensive proximal tubular necrosis without recovery following the ingestion of Amanita phalloides: a case report. *Journal of nephrology, 34*(6), 2137-2140. doi:https://10.1007/s40620-021-01018-w

- Arima, Y., Hirota, T., Bronner, C., Mousli, M., Fujiwara, T., Niwa, S.-i., . . . Saya, H. (2004). Down-regulation of nuclear protein ICBP90 by p53/p21Cip1/WAF1-dependent DNA-damage checkpoint signals contributes to cell cycle arrest at G1/S transition. *Genes to Cells, 9*(2), 131-142. doi:https://doi.org/10.1111/j.1356-9597.2004.00710.x

- Arima, Y., Nitta, M., Kuninaka, S., Zhang, D., Fujiwara, T., Taya, Y., . . . Saya, H. (2005). Transcriptional blockade induces p53-dependent apoptosis associated with translocation of p53 to mitochondria. *Journal of Biological Chemistry, 280*(19), 19166-19176. doi:https://10.1074/jbc.M410691200

- Barbosa, I. A., Machado, N. G., Skildum, A. J., Scott, P. M., & Oliveira, P. J. (2012). Mitochondrial remodeling in cancer metabolism and survival: potential for new therapies. *Biochimica et Biophysica Acta, 1826*(1), 238-254. doi:https://10.1016/j.bbcan.2012.04.005

- Becker, C. E., Tong, T. G., Boerner, U., Roe, R. L., Sco, T. A., MacQuarrie, M. B., & Bartter, F. (1976). Diagnosis and treatment of Amanita phalloides-type mushroom poisoning: use of thioctic acid. *Western Journal of Medicine, 125*(2), 100-109.

- Enjalbert, F., Rapior, S., Nouguier-Soulé, J., Guillon, S., Amouroux, N., & Cabot, C. (2002). Treatment of amatoxin poisoning: 20-year

- retrospective analysis. *Journal of Clinical Toxicology, 40*(6), 715-757. doi:https://10.1081/clt-120014646

- Escudié, L., Francoz, C., Vinel, J. P., Moucari, R., Cournot, M., Paradis, V., . . . Durand, F. (2007). Amanita phalloides poisoning: reassessment of prognostic factors and indications for emergency liver transplantation. *Journal of Hepatology, 46*(3), 466-473. doi:https://10.1016/j.jhep.2006.10.013

- Faulstich, H., Talas, A., & Wellhöner, H. H. (1985). Toxicokinetics of labeled amatoxins in the dog. *Archives of Toxicology, 56*(3), 190-194. doi:https://10.1007/bf00333425

- Fineschi, V., Di Paolo, M., & Centini, F. (1996). Histological criteria for diagnosis of amanita phalloides poisoning. *Journal of Forensic Sciences, 41*(3), 429-432.

- Ganzert, M., Felgenhauer, N., & Zilker, T. (2005). Indication of liver transplantation following amatoxin intoxication. *Journal of Hepatology, 42*(2), 202-209. doi:https://10.1016/j.jhep.2004.10.023

- Garcia, J., Costa, V. M., Carvalho, A. T., Silvestre, R., Duarte, J. A., Dourado, D. F., . . . Carvalho, F. (2015). A breakthrough on Amanita phalloides poisoning: an effective antidotal effect by polymyxin B. *Archives of Toxicology, 89*(12), 2305-2323. doi:https://10.1007/s00204-015-1582-x

- Jan, M. A., Siddiqui, T. S., Ahmed, N., Ul Haq, I., & Khan, Z. (2008). Mushroom poisoning in children: clinical presentation and outcome. *Journal of Ayub Medical College Abbottabad, 20*(2), 99-101.

- Karlson-Stiber, C., & Persson, H. (2003). Cytotoxic fungi--an overview. *Toxicon, 42*(4), 339-349. doi:https://10.1016/s0041-0101(03)00238-1

- Kaya E, H. M., Karahan S, Bayram S, Yaykaşlı KO, Sürmen MG. (2012). Thermostability of Alpha Amanitin in Water and Methanol. *European Journal of Basic Medical Sciences, 2*(4), 106-111. doi:https://doi.org/10.21601/ejbms/9189

- Kaya, E., Karahan, S., Bayram, R., Yaykasli, K. O., Colakoglu, S., & Saritas, A. (2015). Amatoxin and phallotoxin concentration in Amanita phalloides spores and tissues. *Toxicology and Industrial Health, 31*(12), 1172-1177. doi:https://10.1177/0748233713491809

- Kaya, E., Surmen, M. G., Yaykasli, K. O., Karahan, S., Oktay, M., Turan, H., . . . Erdem, H. (2014). Dermal absorption and toxicity of alpha amanitin in mice. *Cutaneous and Ocular Toxicology, 33*(2), 154-160. doi:10.3109/15569527.2013.802697

- Kaya, E., Yilmaz, I., Admis, O., Oktay, M., Bayram, R., Bakirci, S., . . . Colakoglu, S. (2016). Effects of erdosteine on alpha amanitin-induced hepatotoxicity in mice. *Toxin Reviews, 35*(1-2), 4-9. doi:https://10.1080/15569543.2016.1178146

- Kaya, E., Yilmaz, I., Sinirlioglu, Z. A., Karahan, S., Bayram, R., Yaykasli, K. O., . . . Severoglu, Z. (2013). Amanitin and phallotoxin concentration in Amanita phalloides var. alba mushroom. *Toxicon, 76*, 225-233. doi:https://10.1016/j.toxicon.2013.10.008

- Leist, M., Gantner, F., Naumann, H., Bluethmann, H., Vogt, K., Brigelius-Flohé, R., . . . Wendel, A. (1997). Tumor necrosis factor-induced apoptosis during the poisoning of mice with hepatotoxins. *Gastroenterology, 112*(3), 923-934. doi:https://10.1053/gast.1997.v112.pm9041255

- Li, Y., Xi, Y., Tao, G., Xu, G., Yang, Z., Fu, X., . . . Jiang, T. (2020). Sirtuin 1 activation alleviates primary biliary cholangitis via the blocking of the NF-κB signaling pathway. *International Immunopharmacology, 83*, 106386. doi:https://10.1016/j.intimp.2020.106386

- Lindell, T. J., Weinberg, F., Morris, P. W., Roeder, R. G., & Rutter, W. J. (1970). Specific inhibition of nuclear RNA polymerase II by alpha-amanitin. *Science, 170*(3956), 447-449. doi:https://10.1126/science.170.3956.447

- Magdalan, J., Ostrowska, A., Piotrowska, A., Gomułkiewicz, A., Podhorska-Okołów, M., Patrzałek, D., . . . Dziegiel, P. (2010). Benzylpenicillin, acetylcysteine and silibinin as antidotes in human hepatocytes intoxicated with alpha-amanitin. *Experimental*

and Toxicologic Pathology, 62(4), 367-373. doi:https://10.1016/j.etp.2009.05.003

• Magdalan, J., Ostrowska, A., Piotrowska, A., Izykowska, I., Nowak, M., Gomułkiewicz, A., . . . Dziegiel, P. (2010). alpha-Amanitin induced apoptosis in primary cultured dog hepatocytes. Folia Histochemica et Cytobiologica, 48(1), 58-62. doi:https://10.2478/v10042-010-0010-6

• Magdalan, J., Piotrowska, A., Gomułkiewicz, A., Sozański, T., Podhorska-Okołów, M., Szeląg, A., & Dzięgiel, P. (2011). Benzylpenicyllin and acetylcysteine protection from α-amanitin-induced apoptosis in human hepatocyte cultures. Experimental and Toxicologic Pathology, 63(4), 311-315. doi:https://10.1016/j.etp.2010.02.004

• McIlwain, D. R., Berger, T., & Mak, T. W. (2013). Caspase functions in cell death and disease. Cold Spring Harbor perspectives in biology, 5(4), a008656-a008656. doi:https://10.1101/cshperspect.a008656

• Park, R., Choi, W. G., Lee, M. S., Cho, Y. Y., Lee, J. Y., Kang, H. C., . . . Lee, H. S. (2021). Pharmacokinetics of α-amanitin in mice using liquid chromatography-high resolution mass spectrometry and in vitro drug-drug interaction potentials. Journal of Toxicology and Environmental Health, Part A, 84(20), 821-835. doi:https://10.1080/15287394.2021.1944942

• Pišlar, A., Sabotič, J., Šlenc, J., Brzin, J., & Kos, J. (2016). Cytotoxic L-amino-acid oxidases from Amanita phalloides and Clitocybe geotropa induce caspase-dependent apoptosis. Cell Death Discovery, 2(1), 16021. doi:https://10.1038/cddiscovery.2016.21

• Schmittgen, T. D., & Livak, K. J. (2008). Analyzing real-time PCR data by the comparative C(T) method. Nature Protocols, 3(6), 1101-1108. doi:https://10.1038/nprot.2008.73

• Serné, E. H., Toorians, A. W., Gietema, J. A., Bronsveld, W., Haagsma, E. B., & Mulder, P. O. (1996). Amanita phalloides, a potentially lethal mushroom: its clinical presentation and therapeutic options. Netherlands Journal of Medicine, 49(1), 19-23. doi:https://10.1016/0300-2977(95)00096-8

• Smith, M. R., & Davis, R. L. (2016). Mycetismus: a review. Gastroenterology Report (Oxford), 4(2), 107-112. doi:https://10.1093/gastro/gov062

• Tiegs, G., & Horst, A. K. (2022). TNF in the liver: targeting a central player in inflammation. Seminars in Immunopathology, 44(4), 445-459. doi:10.1007/s00281-022-00910-2

• Tong, T. C., Hernandez, M., Richardson, W. H., 3rd, Betten, D. P., Favata, M., Riffenburgh, R. H., . . . Tanen, D. A. (2007). Comparative treatment of alpha-amanitin poisoning with N-acetylcysteine, benzylpenicillin, cimetidine, thioctic acid, and silybin in a murine model. Annals of Emergency Medicine, 50(3), 282-288. doi:https://10.1016/j.annemergmed.2006.12.015

• Vetter, J. (1998). Toxins of Amanita phalloides. Toxicon, 36(1), 13-24. doi:https://10.1016/s0041-0101(97)00074-3

• Wang, M., Chen, Y., Guo, Z., Yang, C., Qi, J., Fu, Y., . . . Wang, Y. (2018). Changes in the mitochondrial proteome in human hepatocytes in response to alpha-amanitin hepatotoxicity. Toxicon, 156, 34-40. doi:https://10.1016/j.toxicon.2018.11.002

• Wieland, T. (1983). The toxic peptides from Amanita mushrooms. International Journal of Peptide Research, 22(3), 257-276. doi:https://10.1111/j.1399-3011.1983.tb02093.x

• Wieland, T., & Faulstich, H. (1978). Amatoxins, phallotoxins, phallolysin, and antamanide: the biologically active components of poisonous Amanita mushrooms. CRC Critical Reviews in Biochemistry, 5(3), 185-260. doi:https://10.3109/10409237809149870

• Yilmaz, I., Ermis, F., Akata, I., & Kaya, E. (2015). A Case Study: What Doses of Amanita phalloides and Amatoxins Are Lethal to Humans? Wilderness & Environmental Medicine, 26(4), 491-496. doi:https://10.1016/j.wem.2015.08.002

• Zhang, C., Wang, C., Tang, S., Sun, Y., Zhao, D., Zhang, S., . . . Xiao, X. (2013). TNFR1/TNF-α and mitochondria interrelated signaling pathway mediates quinocetone-induced apoptosis in HepG2 cells. Food and Chemical Toxicology, 62, 825-838. doi:https://doi.org/10.1016/j.fct.2013.10.022

• Zhao, J., Cao, M., Zhang, J., Sun, Q., Chen, Q., & Yang, Z. R. (2006). Pathological effects of the mushroom toxin alpha-amanitin on BALB/c mice. Peptides, 27(12), 3047-3052. doi:https://10.1016/j.peptides.2006.08.015

• Zhou, H. Q., Liu, W., Wang, J., Huang, Y. Q., Li, P. Y., Zhu, Y., . . . Zhao, Y. L. (2017). Paeoniflorin attenuates ANIT-induced cholestasis by inhibiting apoptosis in vivo via mitochondria-dependent pathway. Biomedicine & Pharmacotherapy, 89, 696-704. doi:https://10.1016/j.biopha.2017.02.084